Adsorption (2008) 14: 265–274
DOI 10.1007/s10450-007-9089-2

Hydrogen adsorption in transition metal carbon nano-structures

Yun Xia Yang · Ranjeet K. Singh · Paul A. Webley

Received: 30 April 2007 / Revised: 28 October 2007 / Accepted: 18 December 2007 / Published online: 23 January 2008

Abstract Templated microporous carbons were synthesized from metal impregnated zeolite Y templates. Scanning Electron Microscopy (SEM) and Transmission Electron Microscopy (TEM) were employed to characterize morphology and structure of the generated carbon materials. The surface area, micro- and meso-pore volumes, as well as the pore size distribution of all the carbon materials were determined by N_2 adsorption at 77 K and correlated to their hydrogen storage capacity. All the hydrogen adsorption isotherms were Type 1 and reversible, indicating physisorption at 77 K. Most templated carbons show good hydrogen storage with the best sample Rh-C having surface area 1817 m^2/g and micropore volume 1.04 cm^3/g, achieving the highest as 8.8 mmol/g hydrogen storage capacity at 77 K, 1 bar. Comparison between activated carbons and synthesized templated carbons revealed that the hydrogen adsorption in the latter carbon samples occurs mainly by pore filling and smaller pores of sizes around 6 Å to 8 Å are filled initially, followed by larger micropores. Overall, hydrogen adsorption was found to be dependent on the micropore volume as well as the pore-size, larger micropore volumes showing higher hydrogen adsorption capacity.

Keywords Carbon nanostructures · Hydrogen storage · Adsorption

Y.X. Yang · R.K. Singh · P.A. Webley (✉)
Department of Chemical Engineering, Monash University, Clayton, VIC 3800, Australia
e-mail: paul.webley@eng.monash.edu.au

1 Introduction

Hydrogen is considered to be an ideal fuel for solving the energy crisis as well as minimizing environmental impact. Four different methods to store hydrogen are currently available: liquid hydrogen (Aceves et al. 2006), compressed gas, metal hydrides (Cooper et al. 2003; Schlapbach and Zuttel 2001; Zuttel 2004) and sorption on different porous materials such as carbon materials (de la Casa-Lillo et al. 2002; Hirscher et al. 2002; Lueking and Yang 2003), zeolites (Yoon 1993), metal organic frameworks (Rosi et al. 2003; Fichtner et al. 2005; Li et al. 2006), and nano-structured metal particle or films. (Hou et al. 2005a; Hou et al. 2005b; Bobet et al. 2004) Cryogenic liquid hydrogen systems experience potential hydrogen losses due to evaporation; compressed hydrogen system exhibit safety problems and are still too large for automotive applications; metal hydrides systems have high weight and cost concerns, and moreover high temperatures are often required to release hydrogen. Chemical hydrogen storage from ammonia-borane (Keaton et al. 2007) shows promising results on dehydrogenation at relatively low temperatures, however, precursor synthesis is yet to be mastered.

Carbon materials have received attention in this area, because of their low density, high surface area, good chemical stability, and amenability to a wide range of processing conditions. Many novel approaches to control the pore structure have been proposed in the literature. Among them, the template carbonization method has gained more attention as it is a feasible method for preparation of well-structured microporous/mesoporous carbons (Joo et al. 2003; Kyotani et al. 1997; Kyotani 2000; Zakhidov et al. 1998). Kyotani et al. synthesized microporous carbons by a template synthesis process using chemical vapor deposition technique (CVD) wherein carbon precursors were infiltrated

into zeolite nano-channels, employing a number of zeolites viz. USY, NaY, Hβ, KL, mordenite (H-form) and ZSM-5 (H-form) as templates and furfuryl alcohol and acrylonitrile as carbon precusors. Highly ordered microporous carbons with three-dimensional regularity and very high surface areas (3600 m^2/g) as well as different pore-structure can be readily synthesized (Ma et al. 2000, 2001, 2002).

Recently, our group (Chen et al. 2007) synthesized microporous carbons from cation exchanged zeolite Y template using butylene and propylene as carbon precursors and studied hydrogen uptake of these samples and achieved promising results at 77 K and 1 bar. Yang et al., have also templated high surface area carbons with β zeolite as template and acetonitrile as precursor and achieved around 6.9% hydrogen adsorption at 77 K and 20 bar (Yang et al. 2006, 2007a, 2007b, 2007c).

In this paper, we describe synthesis of carbon nanostructures containing dispersed transition-metal nano-particles, (viz. Co, Ni, Cu, Ir, Pt, Ag, Rh and Pd) synthesized by adapting the templating method and measured their hydrogen storage at 77 K and 1 bar. Furthermore, we have compared the hydrogen storage capacities of our samples with the commercially available activated carbon as well as their metal-impregnated counterparts.

2 Experimental

2.1 Materials

Activated carbons both metal impregnated (Pt 3% and Pd 3%) as well as plain were procured from Sigma-Aldrich. Zeolite Y (CBV100 $SiO_2/Al_2O_3 = 5.1$) in its sodium form was procured from Zeolyst international. The metal salts used as source were cobalt nitrate, nickel nitrate, copper nitrate, Iridium chloride, Tetra-ammonia platinum nitrate, silver nitrate, rhodium chloride and palladium chloride. Hydrogen gas (grade 5) as well as propylene gas (5% in nitrogen) were purchased from BOC.

2.2 Synthesis of templated carbons

The carbons utilized in this study were synthesized as follows: NaY zeolite powder was impregnated with transition metal salts of interest, using reported procedures (Jiang et al. 2001; Keane 1994, 1995; Matsui et al. 2005) and the resulting zeolites were denoted as MetalY. Metal impregnated zeolite Y powder was then dehydrated by heating to 673 K in a step-wise mode of 50 K under inert nitrogen gas purge followed by infiltrated with an organic precursor, furfuryl alcohol (FA), in a Rotavapor for 24 hours at room temperature. The sample was then centrifuged, dried and polymerized (in a quartz reactor) to further stabilize the organic precursor followed by carbonization of the organic material at 973 K for 4 hours. After carbonization, chemical vapor deposition (CVD) was conducted with propylene gas for 4 hours at a flow rate of approximately 400 ml/min, followed by heat treatment at 1173 K for another 3 hours. The reactor was cooled to ambient temperature and the zeolite carbon composite material was leached by the 48% hydrofluoric acid (Sigma-Aldrich) for 3 hours at room temperature, to remove the zeolite template, followed by washing with deionized water and then drying in a vacuum oven at 303 K for 24 hours. The resulting carbons were denoted as Metal-C, for example Co impregnated carbon was denoted as Co-C, Ir impregnated carbon was denoted as Ir-C and so on.

3 Characterization

The structure of the zeolite/carbon composites and final carbon samples were examined with an X-ray diffractometer (XRD, Philips PW1130 with CuKα radiation $\lambda = 1.5405$ Å) to confirm removal of the zeolite template. The microscopic features of the resulting carbons were observed with a scanning electron microscope (FESEM 6300) as well as transmission electron microscopy (EM420 and JEOL2011). The carbon fraction was determined by combusting the zeolite carbon composite material by heating it in stepwise mode to 1073 K in oxygen gas in a TG/DTA thermogravimetric analyzer (TG Mettler Toledo TGA/SDTA851). The surface area and the pore structure analysis of the samples were performed on a volumetric adsorption analyzer (Micromeritics, USA ASAP 2020). Before adsorption measurements, the samples were out-gassed under vacuum at 623 K. The BET surface area was measured and the micropore volumes were calculated at a relative pressure of 0.15. The corresponding mesopore volume was determined by subtracting the micropore volume from the total pore volume calculated at a relative pressure of 0.995, which we denoted as V_{total}. Pore size distributions (PSDs) were determined using non-local density functional theory (DFT) for slit-pore like geometry. Hydrogen adsorption isotherms at 77 K were measured using an ASAP 2010 Gas Adsorption Analyzer (Micromeritics, USA). All the samples were degassed at 623 K under vacuum prior to use.

4 Results and discussion

4.1 X-ray analysis

The powder x-ray diffraction (PXRD) patterns for the final carbons are shown in Fig. 1. The peaks corresponding to the parent zeolite template (i.e. metal impregnated Y) are absent, indicating that the entire template has been completely removed by the leaching process. The XRD patterns

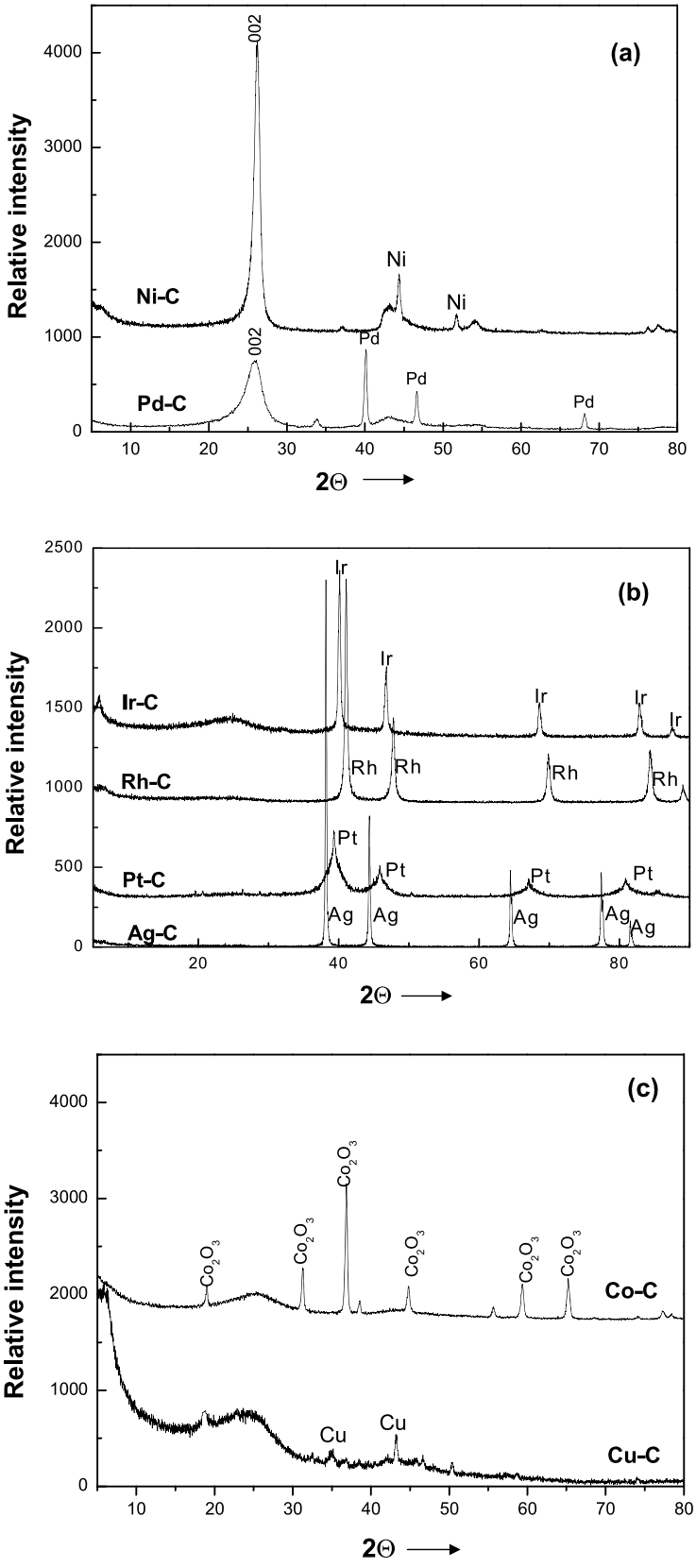

Fig. 1 XRD patterns for the final carbon samples: (**a**) Ni-C and Pd-C (**b**) Ir-C, Pt-C, Ag-C and Rh-C. (**c**) Co-C and Cu-C

Table 1 BET surface area, pore volumes, carbon fraction and hydrogen adsorption data of synthesized carbons

Sample	BET (m^2/g)	V_{total} (cm^3/g)	V_{micro} (cm^3/g)	V_{meso} (cm^3/g)	Carbon fraction (wt%)[#]	Hydrogen ads. mmol/g[+]
Co-C	1613	1.2	0.674	0.526	16	8.28
Ni-C	309	0.25	0.13	0.12	45.6	1.48
Cu-C	1595	1.0	0.672	0.33	25	7.99
Rh-C	1817	1.036	0.758	0.278	23	8.8
Pd-C	197	0.44	0.08	0.36	67	0.95
Ag-C	1267	0.78	0.528	0.252	20.6	4.15
Ir-C	2044	1.12	0.85	0.27	26.3	8.2
Pt-C	911	0.52	0.377	0.321	22.7	4.46
AC*	994	0.468	0.422	0.046	–	7.80
C blank	537	0.59	0.24		20%	2.8
AC+3%Pt*	712	0.667	0.3	0.367	–	6.91
AC+3%Pd*	783	0.72	0.3	0.42	–	6.82

*commercial

#determined from combustion of zeolite carbon composite in oxygen

+hydrogen adsorption at 77 K and 1 bar

for Ni-C and Pd-C samples (Fig. 1a), show high intensity peak at $2\theta \approx 26°$, the intensity being higher in the former sample suggesting presence of graphitic layers formed due to deposition of carbon in form of layers or stacks (graphitization) on the external surface of the zeolite, during the heat treatment, eventually resulting in higher carbon fractions in these samples (Table 1). Ir-C, Pt-C, Ag-C, and Rh-C samples (Fig. 1b) as well as Co-C and Cu-C samples (Fig. 1c) show a small peak at $2\theta \approx 6$, corresponding to the {111} planes of zeolite Y, suggesting that a certain degree of regularity with a periodicity of about 1.4 nm is replicated and well templated morphologies have been retained to a certain extent in these carbons, (Kyotani 2000). Carbons prepared from Ir, Pt, Ag and Rh impregnated Y zeolite templates show a very small peak at 26° showing the absence of graphitic type structures suggesting that these metals may be a less effective catalyst for graphitic type carbon deposition (or nanotube formation) as compared to Ni and Pd and moreover the carbon is deposited inside the pores and channels of the zeolite crystal, leading to formation of microporous carbons and overall moderate carbon fraction (20–26 wt%, Table 1).

Co-C and Cu-C (Fig. 1c), also show relatively broad peak and low intensity peak at $2\theta \approx 26$ (as compared to Ni-C and Pd-C samples, Fig. 1a) suggesting some graphitization. Cu-C shows a more apparent peak at 6°, showing the presence of microporous templated carbon (Kyotani 2000; Chen et al. 2007). However, it should be noted that the peaks in the XRD pattern are relative, and metal particles in other samples show stronger peaks thus reducing or masking the low intensity peaks (typically the 6° peak) in the case of fully templated carbon (Fig. 1b).

Additionally, all the samples show peaks corresponding to respective metal nanoparticles in their reduced state, except for Co-C, wherein a peak corresponding to cobalt oxide is observed. The sizes of the nanoparticles were calculated from the Scherrer equation, and Ni nanoparticle was found to be around 19 nm, Pd 24 nm, cobalt oxide 30 nm, copper 2 nm, Ir 25 nm, Pt 4–6 nm (Yang et al. 2007c), Ag 40 nm and Rh 20 nm.

4.2 Scanning Electron Microscopy

Representative SEM micrographs of the samples with nanotubes (Pd-C), partially templated (Co-C) and completely templated carbons (Ir-C) are shown in Fig. 2a, b and c respectively. According to the SEM images both Pd-C and Ni-C show graphitic structures also supported by the presence of graphitic peak at 26° in the XRD pattern as well as the higher carbon fraction (Table 1). Pd-C (Fig. 2a) sample shows graphitic nanofibers as well as cone helixes, which we will be discussing in more detail elsewhere (Yang et al. 2007c). Similarly, Ni-C shows fiber-like carbon nanotubes (CNT) and spherical carbon onions (CO) (described in TEM section). Metals such as Co and Ni are known to be most active catalysts in carbon nanotube formation and additionally Ni is also known to increase the yield of carbon nanotubes (Ciambelli et al. 2005; Yudasaka et al. 1995; Baker et al. 1972). The Co-C (Fig. 2b) sample is mainly comprised of partially templated carbon and very small amount of CNTs as compared to Ni-C. This observation is contrary

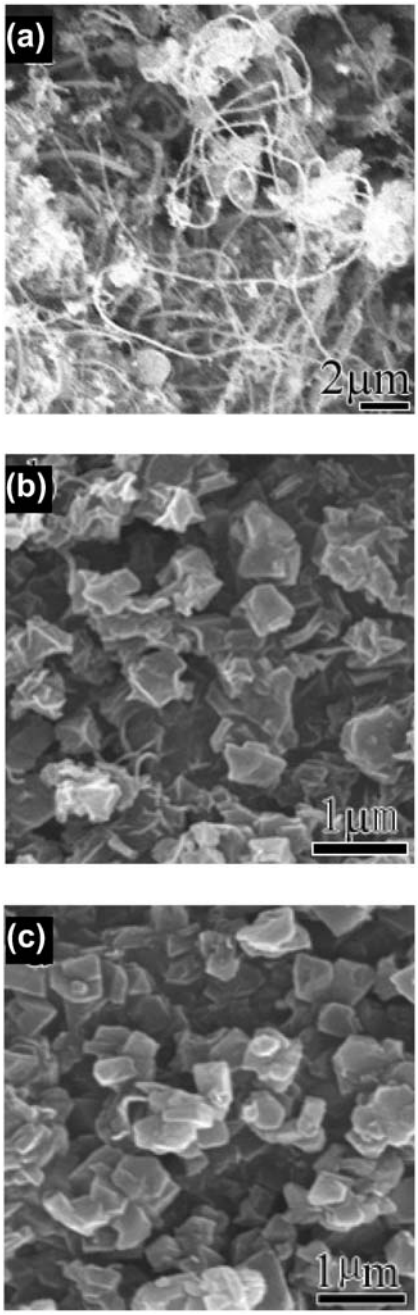

Fig. 2 Scanning electron microscopy images of (**a**) Pd-C (**b**) Co-C and (**c**) Ir-C samples

to Ciambelli et al. (2005), wherein they generated nanotubes with 70% selectivity from Co-Beta zeolite as template. In our case, under our synthesis conditions Co salts were oxidized to cobalt oxides rather than reduced to metallic Co (Fig. 1c); hence Co was not available in its metallic form for nanotube formation resulting in partially templated carbon. CuY-C (shown in supporting information) has similar morphology as CoY-C (partially templated), and shows negligible nanotubes. Copper metal is known to be a poor catalyst for catalytic conversion and generally does not produce nanotube type carbon structures (Ciambelli et al. 2005). On the other hand, Ir-C, Pt-C, Ag-C and Rh-C retain the morphology of parent zeolite Y templates suggesting that these metals facilitate carbonization and polymerization of carbons inside the zeolite pore structures leading to microporous carbons. SEM images are provided in the supporting information file. The SEM of Ir-C (Fig. 2c) sample is shown as a representative of this group. The smooth surface of these carbons emphasizes the fact that most of the carbon was deposited inside the zeolite channels (Hou et al. 2005a).

4.3 Nitrogen adsorption and pore size distribution

Figure 3 shows the N_2 adsorption isotherms at 77 K for some of the carbon samples synthesized in this work. Graphitic carbons or carbons with nanotubes viz. Ni-C (Fig. 3) and Pd-C behaved alike and show very low N_2 adsorption, hence low surface area (Table 1) as expected indicating less micropores. All the other carbons partially templated (Co-C and Cu-C) or fully templated (Ir-C, Rh-C and Ag-C) show type I isotherms and high surface area $>1000\ m^2/g$ (Table 1) except Pt-C which has slightly lower surface area. The very sharp adsorption isotherm suggests that the samples have larger micro-pore volume. Both partially and fully templated carbon samples show a minor hysteresis during desorption suggesting the presence of mesoporosity to a certain extent. Commercial activated carbon shows no hysteresis, however, their metal impregnated counterparts show lower surface areas and develop some mesoporosity (Fig. 3, Act-3% Pt), suggesting possible blockage of pores by metals or collapse of weak carbon linkages during synthesis leading to mesopores.

Figure 4 shows the pore size distribution (PSDs) for Ni-C representing the graphitic carbons; Ir-C Rh-C and Pt-C form fully templated carbons as well as Co-C and Cu-C which are partially templated carbons. Activated carbon (not shown) shows a very high micropore volume ($\sim 0.17\ cm^3/g$) at 5.8 Å, while metal impregnated activated carbons showed relatively lower micropore volumes at 6.7 Å ($0.08\ cm^3/g$) in case of Pd and at 7.3 Å ($0.08\ cm^3/g$) in case of Pt, again pointing to blocked micropores by the metal particles making them inaccessible to adsorbate gases.

All the carbon samples show bimodal pore size distribution, the first low intensity peak typically in the 6–8 Å range and second high intensity peak at about 12 Å. Pore sizes at 12 Å are very close to the *d*-spacing of 6° on XRD pattern corresponding to the super-cage size 14 Å in zeolite Y framework, suggesting the presence of long range ordered structure in all of these carbon samples. Additionally all samples show mesoporosity to a certain degree, suggesting partial carbon deposition or collapse of weakly linked carbon during the heat treatment and leaching processes (Chen et al. 2007). Pore size distribution of graphitic carbons Ni-C and Pd-C show low micropore volumes as these

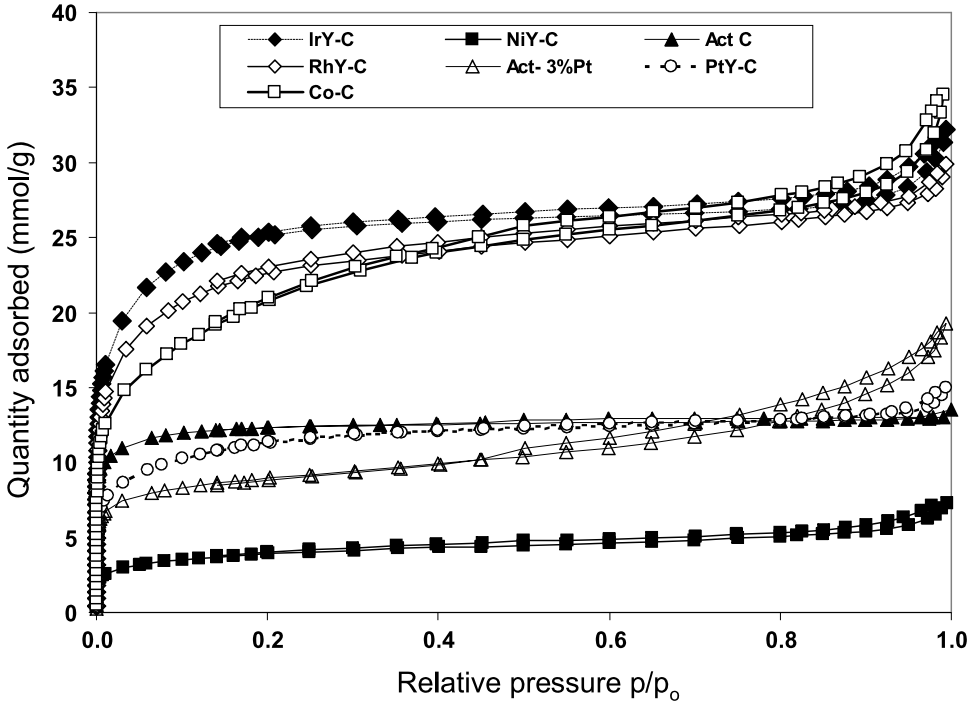

Fig. 3 Nitrogen adsorption isotherms at 77 K and 1 bar of the synthesized as well as commercial activated carbons

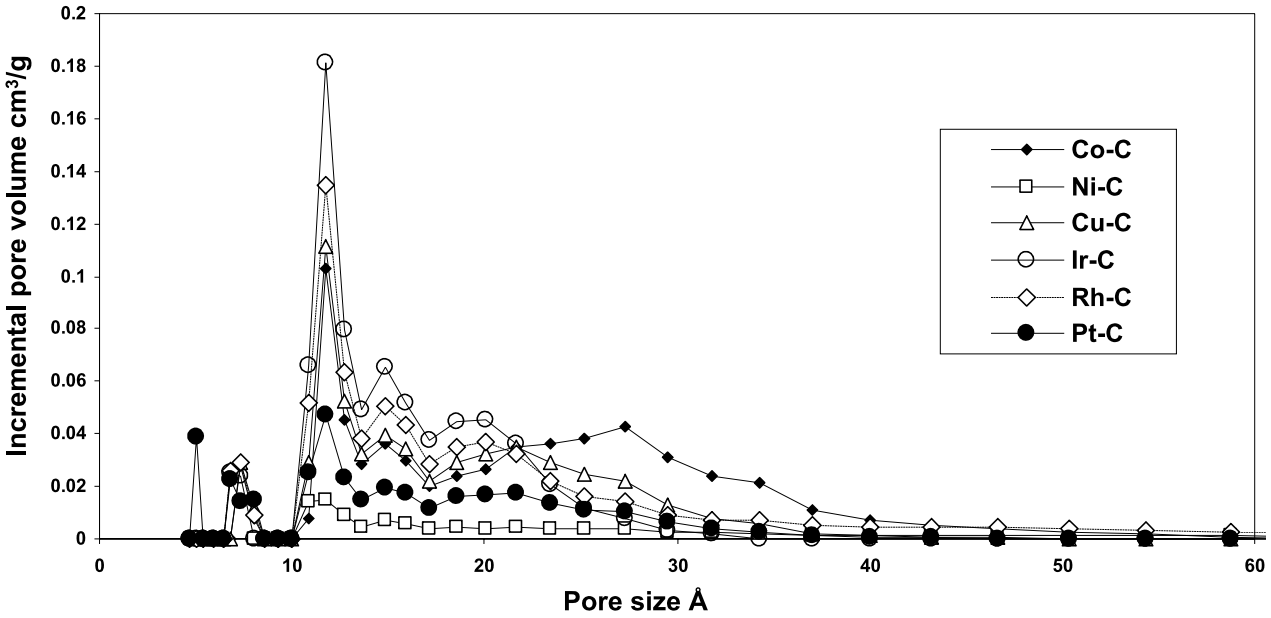

Fig. 4 Pore size distribution on different types of synthesized carbons

carbons mainly contain nanotubes as displayed in SEM images, XRD patterns (Fig. 1a) as well as very low surface area (Table 1). Co-C and Cu-C samples, which have retained partial zeolite template structure, show more or less similar pore volumes and pore size distribution; however, Co-C sample showed more pores in the mesopore range as compared to the Cu-C sample (Fig. 4; Table 1) suggesting that Co in its oxide form is an inactive catalyst for hydrocarbon conversion as compared to Cu metal resulting in partial deposition of the carbon inside the pores, leading to generation of voids in the structure, which is also reflected in its low carbon fraction. Rh-C and Ir-C (Fig. 4) on the other hand show high micropore volume in the range 6–8 Å and at 12 Å, the latter sample showing the highest, followed by Rh-C, Cu-C, Co-C (Fig. 4) and Ag-C sample, suggesting that Rh, Ir, Ag and Pt catalyze hydrocarbon carbonization leading to well templated ordered microporous carbons. Pt-C samples shows an additional peak at 5 Å which may be attributed to loss of

small volatiles such as CO_2, H_2O and H_2 given out during the heat treatment process (Chen et al. 2007).

4.4 Transmission Electron Microscopy

Representative transmission electron microscopy images for Ni-C as an example of graphitic carbons and Rh-C as an example of templated carbons are shown in Fig. 5a and b respectively. Ni-C samples are comprised of nanofibers (NF) and carbon onions (CO) with inset showing the layered structure of CO (shown in Fig. 5a and supporting information file). Rh-C, Ag-C, Ir-C samples show very long range ordered structure with periodicity of 1.4 nm suggesting the template structure was replicated, the dark spots in the TEM correspond to the metal nanoparticles and their sizes are described earlier. (TEMs are shown in supporting information)

4.5 Hydrogen adsorption

Hydrogen adsorption isotherms for all the carbon samples are shown in Fig. 6 and their hydrogen adsorption capacities are summarized in Table 1. DFT analysis of commercial activated carbon, as well as commercial carbons with 3% Pt and Pd show high micropore volumes at 6 Å, 7 Å, and 8 Å, respectively. Correspondingly, their hydrogen isotherms show high adsorption in the low-pressure range (below 20 kPa), which tend to saturate with increase in pressure (120 kPa). In the case of partially templated (Co-C and Cu-C) as well as fully templated carbons (Rh-C and Ir-C), the hydrogen isotherm shows a gradual increase with increase in pressure suggesting that the smallest pores are

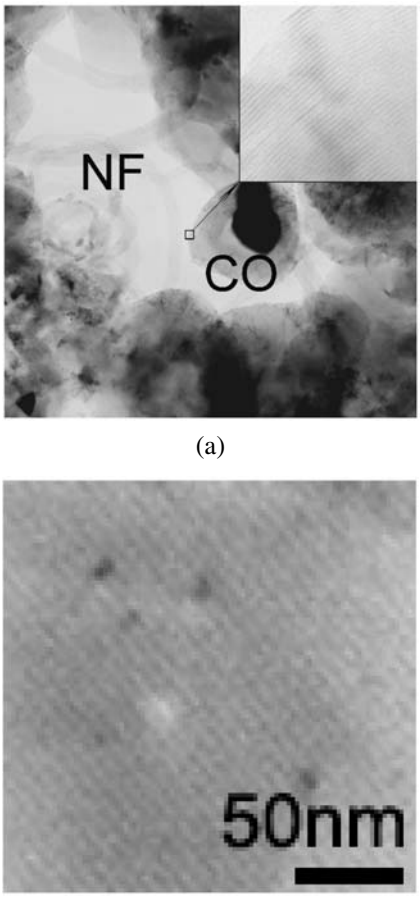

(a)

(b)

Fig. 5 TEM images for (**a**) Ni-C and (**b**) Rh-C samples

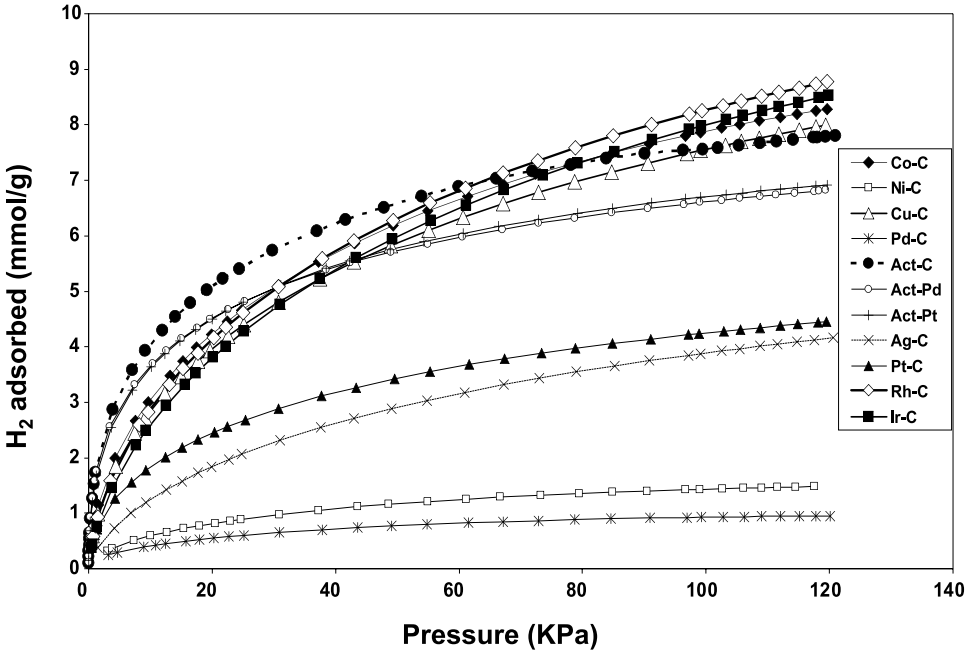

Fig. 6 Hydrogen adsorption isotherm at 77 K and 120 kPa on the synthesized samples and commercial carbon samples

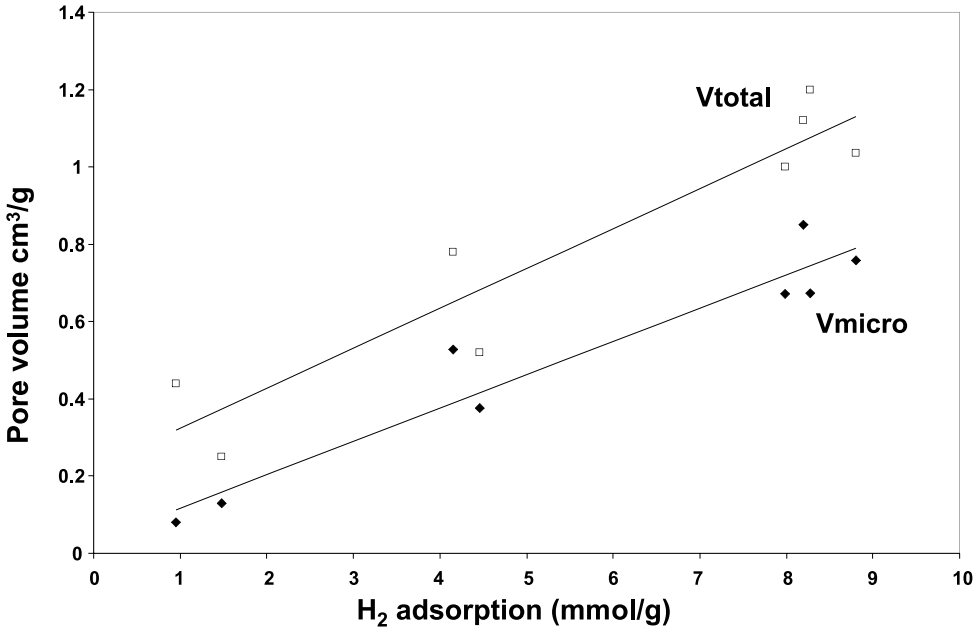

Fig. 7 Relationship between hydrogen adsorption and pore volumes for synthesized carbons

filled initially (<10 Å) followed by the larger micropores. It should be noted that Rh-C, Ir-C, Cu-C and Co-C have more or less similar pore volumes at pore-size 6–8 Å and show nearly similar hydrogen uptake (8.0–8.8 mmole/g; Table 1). Although, the pore volume of Ir-C at ∼12 Å is highest (Fig. 4; Table 1), Rh-C shows the highest H_2 uptake. Ir-C has slightly lower pore volume in the smaller pore range (6–8 Å) as compared to Rh-C, which may be reflected in the difference between their H_2 uptakes, however, this difference is very subtle and well within experimental error. Pt-C carbons show slightly higher and steeper adsorption isotherms as compared to Ag-C carbon sample, although the latter has higher surface area. DFT analysis of Pt-C carbon shows a pore volume at 5 Å (Fig. 4) suggesting smaller pores, similar to commercial activated carbons although the pore volume is lower. These smaller pores fill up initially as supported by a sharp adsorption isotherm in case of Pt-C as compared to Ag-C and then saturates, while the hydrogen uptake in Ag-C carbons seems to increase (similar to Rh-C, Ir-C, Co-C and Cu-C) and may adsorb more H_2 than Pt-C at higher pressure (>120 kPa). Nanotubes or graphitic materials show very low hydrogen uptake, which is expected, as their micropore volumes are low.

Overall in the case of fully templated (except Pt-C) and partially templated carbons, measurements at 77 K demonstrate that they are far from their saturation limits for H_2 adsorption. Additionally we believe that the H_2 molecules are adsorbed predominantly by smaller pores in range 6 Å to 8 Å, in agreement with Jagiello et al. (2006), followed by pores >10 Å.

The relationship between hydrogen adsorption capacities (77 K and 1 bar) and micropore volume (denoted as V_{micro}) as well as the total pore volumes is shown in Fig. 7. There is an approximate linear relationship between hydrogen adsorption capacity and micropore volume (V_{micro}) as well as the total pore volume, in contrast to reports by Jordá-Beneyto et al. (2007) wherein pore-size distribution appeared to have no impact on hydrogen adsorption at 77 K in the case of activated carbons. In our samples the micropore volume and PSD appears to play some role in the overall hydrogen adsorption and especially pores <10 Å seem to be responsible for hydrogen adsorption (Jagiello et al. 2006; Nijkamp et al. 2001). Mesopore volume appears to play a less important role in hydrogen adsorption.

Moreover, impregnated metal did not appear to play role in hydrogen chemisorption (beyond their role in directing the PSD) because all the hydrogen isotherms were found to be fully reversible and no evidence of spill-over phenomena was observed.

5 Conclusion

Templated metal impregnated carbons have been synthesized. Although zeolite Y was used as template for all the carbons, the resulting carbon structure was sensitive to the type of impregnated metal. Ni and Pd impregnated templates produced nanotubes and nanofibres while other metals produced partially or fully templated microporous carbons. SEM and TEM confirmed that the templated morphology is fully or partially retained and also revealed that the generated carbons contain dispersed metal nanoparticles of sizes varying from 2 nm to 20 nm. Surface area results indicate that all the templated carbon samples (except samples with nanotubes and nanofibres) pos-

sess high surface area and micro-pore volume with bimodal pore-size distribution at 6–8 Å and 12 Å respectively, the latter pointing to the fact that regularity and order of zeolite Y template structure is well replicated in the final carbons. Hydrogen adsorption isotherms for the carbon samples investigated were type I and reversible, suggesting physisorption and metal particles played no part in hydrogen chemi-sorption. Hydrogen adsorption was found to be approximately more linearly dependent on micropore volume as well as the pore-size than total pore volume, with higher micro-pore volumes giving higher hydrogen adsorption. Smaller pore sizes leading to sharper hydrogen adsorption isotherm increases at zero loading.

Acknowledgements Authors would like to thank Professor Dong Yuan Zhao from Fudan University, China for SEM analysis and Monash University for financial support.

References

Aceves, S.M., Berry, G.D., Martinez-Frias, J., Espinosa-Loza, F.: Vehicular storage of hydrogen in insulated pressure vessels. Int. J. Hydrog. Energy **31**, 2274–2283 (2006)

Baker, R.T.K., Barber, M.A., Waite, R.J., Harris, P.S., Feates, F.S.: Nucleation and growth of carbon deposits from nickel catalyzed decomposition of acetylene. J. Catal. **26**, 51 (1972)

Bobet, J.L., Grigorova, E., Khrussanova, M., Khristov, M., Stefanov, P., Peshev, P., Radev, D.: Hydrogen sorption properties of graphite-modified magnesium nanocomposites prepared by ball-milling. J. Alloys Comp. **366**, 298–302 (2004)

Chen, L., Singh, R.K., Webley, P.: Synthesis, characterization and hydrogen storage properties of microporous carbons templated by cation exchanged forms of zeolite Y with propylene and butylene as carbon precursors. Microporous Mesoporous Mat. **102**, 159–170 (2007)

Ciambelli, P., Sannino, D., Sarno, M., Fonseca, A., Nagy, J.B.: Selective formation of carbon nanotubes over co-modified beta zeolite by CCVD. Carbon **43**, 631–640 (2005)

Cooper, A., Charls, G., Pez, P.: Hydrogen storage using carbon-metal hybrid compositions. US Patent 6,596,055 (2003)

de la Casa-Lillo, M.A.F., Cazorla-Amoros, L.-D., Linares-Solano, A.: Hydrogen storage in activated carbons and activated carbon fibers. J. Phys. Chem. B **106**, 10930–10934 (2002)

Fichtner, M.: Nanotechnological aspects in materials for hydrogen storage. Adv. Eng. Mat. **7**, 443–455 (2005)

Hirscher, M., Becher, M., Haluska, M., Quintel, A., Skakalova, V., Choi, Y.-M., Dettlaff-Weglikowska, U., Roth, S., Stepanek, I., Bernier, P., Leonhardt, A., Fink, J.: Hydrogen storage in carbon nanostructures. J. Alloys Comp. **330**, 654–658 (2002)

Hou, Y., Kondoh, H., Ohta, T., Gao, S.: Size-controlled synthesis of nickel nanoparticles. Appl. Surf. Sci. **241**, 218–222 (2005a)

Hou, P.X., Yamazaki, T., Orikasa, H., Kyotani, T.: An easy method for the synthesis of ordered microporous carbons by the template technique. Carbon **43**, 2624–2627 (2005b)

Jagiello, J., Anson, A., Martinez, M.T.: DFT-based prediction of high-pressure H-2 adsorption on porous carbons at ambient temperatures from low-pressure adsorption data measured at 77 K. J. Phys. Chem. B **110**, 4531–4534 (2006)

Jiang, Y.X., Sun, S.G., Ding, N.: Novel phenomenon of enhancement of IR absorption of CO adsorbed on nanoparticles of Pd confined in supercages of Y-zeolite. Chem. Phys. Lett. **344**, 463–470 (2001)

Jorda-Beneyto, M., Suarez-Garcia, F., Lozano-Castello, D., Cazorla-Amoros, D., Linares-Solano, A.: Hydrogen storage on chemically activated carbons and carbon nanomaterials at high pressures. Carbon **45**, 293–303 (2007)

Joo, S.H., Ryoo, R., Kruk, M., Jaroniec, M.: Thermally induced structural changes in SBA-15 and MSU-H silicas and their implications for synthesis of ordered mesoporous carbons. Stud. Surf. Sci. Catal. **146**, 49–52 (2003)

Keane, M.A.: Role of the alkali metal co-cation in the ion exchange of Y zeolites I. Alkali metal and nickle ion-exchange equilibria. Microporous Mat. **3**, 93–108 (1994)

Keane, M.A.: Role of the alkali metal co-cation in the ion exchange of Y zeolites II. Copper ion-exchange equiliria. Microporous Mat. **4**, 385–394 (1995)

Keaton, R.J., Blacqulere, J.M., Baker, R.T.: Base metal catalyzed behydrogenation of ammonia-borane for chemical hydrogen storage. J. Am. Chem. Soc. **129**, 1844–1845 (2007)

Kyotani, T.: Control of pore structure in carbon. Carbon **38**, 269–286 (2000)

Kyotani, T., Nagai, T., Inoue, S., Tomita, A.: Formation of new type of porous carbon by carbonization in zeolite nanochannels. Chem. Mat. **9**, 609–615 (1997)

Li, Y.W., Yang, R.T.: Hydrogen storage in metal-organic frameworks by bridged hydrogen spillover. J. Am. Chem. Soc. **128**, 8136–8137 (2006)

Lueking, A., Yang, R.T.: Hydrogen storage in carbon nanotubes: Residual metal content and pretreatment temperature. Aiche J. **49**, 1556–1568 (2003)

Nijkamp, M.G., Raaymakers, J., van Dillen, A.J., de Jong, K.P.: Hydrogen storage using physisorption—materials demands. Appl. Phys. Mat. Sci. Proces. **72**, 619–623 (2001)

Ma, Z.X., Kyotani, T., Tomita, A.: Preparation of a high surface area microporous carbon having the structural regularity of Y zeolite. Phys. Chem. Chem. Phys. **2**, 2365–2366 (2000)

Ma, Z.X., Kyotani, T., Liu, Z., Terasaki, O., Tomita, A.: Very high surface area microporous carbon with a three-dimensional nano-array structure: Synthesis and its molecular structure. Chem. Mater. **13**, 4413–4415 (2001)

Ma, Z., Takashi, K., Tomita, A.: Synthesis methods for preparing microporous carbons with a structural regularity of zeolite Y. Carbon 2367–2374 (2002)

Matsui, T., Harada, M., Ichihashi, Y., Bando, K.K., Matsubayashi, N., Toba, M., Yoshimura, Y.: Effect of noble metal particle size on the sulfur tolerance of monometallic Pd and Pt catalysts supported on high-silica USY zeolite. Appl. Catal. A Gen. **286**, 249–257 (2005)

Rosi, N.L., Eckert, J., Eddaoudi, M., Vodak, D.T., Kim, J., O'Keeffe, M., Yaghi, O.M.: Hydrogen storage in microporous metal-organic frameworks. Science **300**, 1127–1129 (2003)

Schlapbach, L., Zuttel, A.: Hydrogen-storage materials for mobile applications. Nature **414**, 353–358 (2001)

Yang, Z.X., Xia, Y.D., Sun, X.Z., Mokaya, R.: Preparation and hydrogen storage properties of zeolite-templated carbon materials nanocast via chemical vapor deposition: Effect of the zeolite template and nitrogen doping. J. Phys. Chem. B **110**, 18424–18431 (2006)

Yang, Y.X., Lee, W.J., Zhao, D., Webley, P.A.: Template synthesis of ordered microporous carbons containing well dispersed Platinum nanoparticles. Adv. Func. Mat. (2007a, submitted)

Yang, Y., Rosalie, J., Bourgeois, L., Webley, P.A.: Bulk synthesis of carbon nanostructures: hollow stacked-cone-helices by chemical vapor deposition. Mat. Res. Bull. (2007b). doi:10.1016/j.materresbull.2007.08.020

Yang, Z., Xia, Y., Mokaya, R.: Enhanced hydrogen storage capacity of high surface area zeolite-like carbon materials. J. Am. Chem. Soc. **129**, 1673–1679 (2007c)

Yoon, J.-H.: Pressure-dependent hydrogen encapsulation in Na12-zeolite. A. J. Phys. Chem. 6066–6068 (1993)

Yudasaka, M., Kikuchi, R., Matsui, T., Ohki, Y., Yoshimura, S., Ota, E.: Specific conditions for Ni catalyzed carbon nanotube growth by chemical-vapor-deposition. Appl. Phys. Lett. **67**, 2477–2479 (1995)

Zakhidov, A.A., Baughman, R.H., Iqbal, Z., Cui, C.X., Khayrullin, I., Dantas, S.O., Marti, I., Ralchenko, V.G.: Carbon structures with three-dimensional periodicity at optical wavelengths. Science **282**, 897–901 (1998)

Zuttel, A.: Hydrogen storage methods. Nature **91**, 157–172 (2004)